HEALING OF FRACTURES IN ROCK SALT

Kittitep Fuenkajorn

Received: Apr 18, 2006; Revised: Aug 3, 2006; Accepted: Aug 7, 2006

Abstract

Healing effectiveness of rock salt fractures as affected by the applied stresses, fracture characteristics, moisture content and time was investigated in the laboratory. The effort involved (1) fracture pressurization tests under uniaxial and radial loading, (2) gas flow permeability tests to monitor the time-dependent behavior of the salt fractures, and (3) point loading and diameter loading tests to assess the mechanical performance of the fractures after healing. Tension-induced fractures and fractures formed by saw-cut surfaces and by polished surfaces were prepared in salt specimens. Series of gas flow testing were performed to monitor the changes of the fracture permeability under quasi-static loading ranging from 0.7 to 20 MPa for up to 120 h. Healing tests under static loading are were carried out under both dry and saturated conditions. The results suggest that the primary factors governing the healing of salt fractures are the origin and purity of the fractures, and the magnitude and duration of the fracture pressurization. Inclusions or impurities significantly reduce the healing effectiveness. The hydraulic conductivity of the fractures in pure salt can be reduced permanently by more than 4 orders of magnitude under the applied stress of 20 MPa for a relatively short period. For most cases the reduction of salt fracture permeability is due to the fracture closure which does not always lead to fracture healing. The closure involves visco-plastic deformation of the asperities on both sides of the salt fracture, while the healing is related to the covalent bonding between the two surfaces. Fracture roughness and brine saturation apparently have an insignificant impact on the healing process.

Keywords: Healing, rock salt, fracture, permeability

Introduction

Damage or fractures in rock salt formations can be healed under hydrostatic and non-hydrostatic compression. When cracks are closed, permeability can be reduced by several orders of magnitude (Renard, 1999). The healing capability of fractures is one of the advantages for rock salt to be used as a host rock for nuclear waste repository in the United States and Germany (Habib and Berest, 1993). The presence of damage in the form of micro-cracks in salt can alter the structural stability and permeability of salt, affecting the integrity of a repository (Chan *et al*., 1998). The healing of rock salt fractures around air or gas storage caverns also affects the designed storage capacity and the mechanical stability of the caverns (Katz and Lady, 1976).

Geomechanics Research Unit, Institute of Engineering, Suranaree University of Technology, Nakhon Ratchasima 30000, Thailand. Tel: 0-4422-4443, Fax: 0-4422-4448, E-mail: kittitep@sut.ac.th
[*] *Corresponding author*

Suranaree J. Sci. Technol. 13(4):307-316

Miao *et al*. (1995) state that healing of rock salt is probably due to the visco-plastic deformation of grains, causing the closure of cracks and pore spaces. The size reduction of the micro-cracks can increase the salt stiffness and strength. The main driving force for fracture healing is a minimization of surface tension, and creation of contact areas and covalent bonds between the two surfaces of the fracture.

It is defined here that healing is the closure of fractures without any precipitation of materials inside. It is a chemical and physical process in which the material properties evolve with time or in which the defects (voids and cracks) decrease. The initiation, propagation and healing of fractures in salt mass around underground structures have long been recognized; most investigations however have concentrated on their impact on the mechanical constitutive behavior of the rock (e.g., Allemandou and Dusseault, 1993; Munson *et al*., 1999). Several experimental researches on the healing and consolidation of crushed salt have also been carried out in an attempt at understanding the healing behavior between the salt particles and their impact on the bulk properties (e.g., Ouyang and Daemen, 1989; Miao *et al*., 1995). A direct experimental assessment of the healing behavior of individual salt fractures remains rare.

The objective of this research is to assess experimentally the healing effectiveness of rock salt fractures as affected by the stress conditions, fracture types, and time. The effort involved healing tests under uniaxial and radial pressures, gas flow permeability tests to monitor the time-dependent behavior of the salt fractures, and point loading and diameter loading tests to assess the mechanical performance of the fractures after healing.

Salt Specimens

The salt specimens used here were drilled from the Middle and Lower members of the Maha Sarakham Formation in the Sakhon Nakhon Basin, northeastern Thailand. Warren (1999) and Suwanich (1986) gave detailed descriptions of the salt and geology of the basin. The core specimens were from depths ranging between 250 m and 400 m of drillhole no.BD99-1. The drilling was carried out by the Asia Pacific Potash Corporation. The compressive and tensile strengths of the salt were determined. These properties were needed for designing the healing test parameters. The nominal diameter of all specimens was 60 mm. The sample preparation and test procedures followed as much as practical the ASTM standard practices (i.e., ASTM D2938, D3967, D4543 and D5731). Table 1 summarizes the test results.

Fracture Healing Experiments

Two loading schemes were employed to assess the healing behavior of the salt fractures: uniaxial (normal) loading, and radial loading. Three types of salt fractures were simulated in the laboratory: 1) tension-induced fractures, 2) fractures formed by saw-cut surfaces, and 3) fractures formed by smooth polished surfaces. All fractures were well mated. All tests were carried out under isothermal conditions (22 - 25^{o}C). To obtain the tension-induced fractures, the cylindrical specimens were subjected to point loading or diameter loading (Brazilian tension test). The point-loaded fracture was normal to the specimen axis, and was prepared for healing under uniaxial loading. The diameter-loaded fracture was parallel to the specimen axis, and was healed

Table 1. Summary of characterization test results

Salt member	Depth (m)	Test methods		
		Uniaxial strength, σ_c	Brazilian strength, σ_B	Point load strength, I_s
Middle Salt	252 - 329	30.2 ± 4.2 MPa	1.9 ± 0.3 MPa	1.0 ± 0.01 MPa
Lower Salt	390 - 410	31.1 ± 6.7 MPa	1.7 ± 0.3 MPa	0.6 ± 0.05 MPa

under radial loading. The fracture formed by saw-cut surfaces was also normal to the specimen axis, while the fracture formed by polished surfaces was parallel to the specimen axis. Prior to pressurization the types and amounts of inclusions on the fracture surfaces were determined and mapped. The aerial percentage of the inclusions was calculated with respect to the total fracture area. These inclusions included all associated and foreign minerals or materials that were not sodium chloride.

Healing Under Normal Load

Four test series with different test conditions were performed on the saw-cut fractures. For the first two series, the normal stresses of 3.2 kPa and 3.8 kPa were applied to the saw-cut fractures under dry and saturated conditions, respectively. Three specimens were used for each normal stress. A dead weight compression machine applied constant loading onto the fracture (Figure 1). For the saturated condition, the fractures were submerged under saturated brine while loading. The load was removed after 30 days. No healing was observed for both dry and saturated fractures. All saw-cut fractures remained separable.

The third and fourth test series used a normal stress of 4.3 MPa on three saw-cut fractures, and 7.8 MPa on ten tension-induced fractures. A consolidation machine with the maximum load capacity of 4 tons was used to apply constant stresses to the specimens for 30 days. The specimens were then subjected to point load testing by having the loading points lied parallel to the healed fracture plane (Figure 2). The point load strength of the healed fracture (I_H) was calculated by dividing the failure load (P) by the diameter square (D^2). The healing effectiveness (H_e) of each fracture is defined by the percentage ratio of I_H to I_S, where I_S represents the point load strength of the intact salt obtained previously from inducing the fracture to the same specimen. All specimens failed along the saw-cut surfaces.

No healing was detected on the saw-cut fractures tested under 4.3 MPa normal stress (test series 3). Healing however was observed on the tension-induced fractures tested under 7.8 MPa normal stress (test series 4). Table 2 summarizes the results. Some H_e values exceeded 100%. This was probably because some existing voids or fissures in salt along the fracture plane were compressed during the healing period,

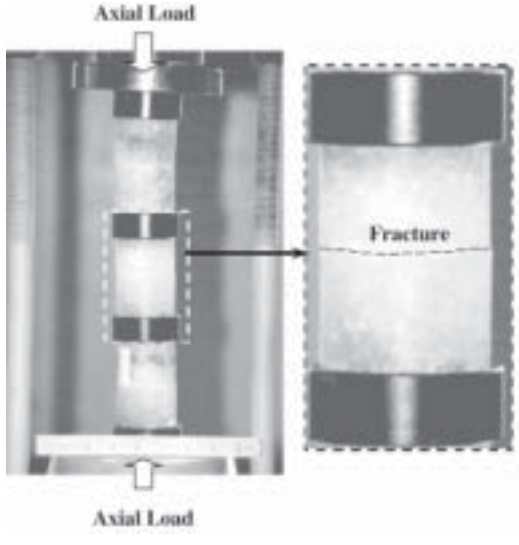

Figure 1. Healing test under uniaxial loading. The specimens are loaded axially by means of a dead weight consolidation machine

subsequently strengthening the fracture beyond the previous intact condition. It should be noted that before the fractures were initially induced, the intact core specimens were not subjected to any compression. The high variation of H_e values is probably due to the nature of the point loading test method. Even though the assessment of healing effectiveness by point load testing is relatively quick and easy, the high stress gradient induced in the specimen usually enhances the intrinsic variability of the measurement results. The complex distribution, pattern and locations of the inclusions in relation to the loading points can also enhance the variability of the strength results. The healing effectiveness tends to decrease as the amount of inclusion increases.

Healing Under Radial Loading

Tension-induced fractures and polished fractures (Figure 3) were tested under radial pressures by using overburden Poro-Perm Cell. Each fracture type was subjected to two loading configurations: static (single-step) loading and quasi-static (multi-step) loading. All specimens were tested under dry conditions. During pressurization, a series of gas flow permeability tests was performed. The measured flow rate was used to calculate the hydraulic conductivity

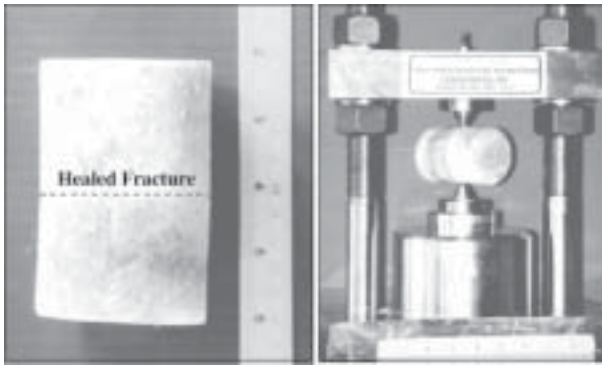

Figure 2. Salt specimen with fracture after healing under uniaxial load (left). The healing effectiveness is assessed by point load testing (right)

Table 2. Point load test results for dry salt specimens with tension-induced fractures after healing under constant normal stress of 7.8 MPa for 30 days

Specimen No.	Inclusions (%)	Point load strength index		Healing effectiveness $H_e = [I_H/I_S] \times 100$ (%)
		Intact salt I_S (MPa)	Salt with healed fracture, I_H (MPa)	
HUT01e	0	0.61	1.13	185
HUT02e	30	1.05	0.75	71
HUT03e	5	0.84	1.00	119
HUT04e	40	1.09	0.40	37
HUT05e	25	0.87	0.74	85
HUT06e	10	0.56	0.59	105
HUT07e	5	1.22	0.49	40
HUT08e	5	1.25	0.48	38
HUT09e	25	0.54	0.51	94
HUT10e	15	0.56	0.40	71

of the fracture (K_f) as a function of time, based on an assumption of the flow through parallel plates (Zeigler, 1976). The nitrogen gas pressure was injected at a constant magnitude of 0.35 MPa. The measurement limit of the system was 10^{-8} m/s.

One polished fracture was subjected to the radial pressure (P_c) of 3.45 MPa which was later increased to 6.89 MPa (quasi-static loading). Each loading took 100 h. This pressure scheme was repeated for the second cycle. The fracture permeability decreased with increasing radial pressures (Figure 4). Under each load, the fracture permeability also decreased with time. The second cycle of pressurization yields a lower hydraulic conductivity than did the first one, which suggested a plastic closure of the fracture. When the pressure increased to 6.89 MPa, the hydraulic conductivity dropped below the limit of measurement (10^{-8} m/s).

Three tension-induced fractures were tested under quasi-static loading. The constant radial pressures were progressively increased from 3.45, 6.89, 10.34 to 13.78 MPa. The reduction of fracture permeability with time and pressurization was found to be greater than that of the polished fracture. The permeability obtained from the second pressure cycle was notably lower than that of the first one, suggesting a significant closure of the fracture. Figure 5

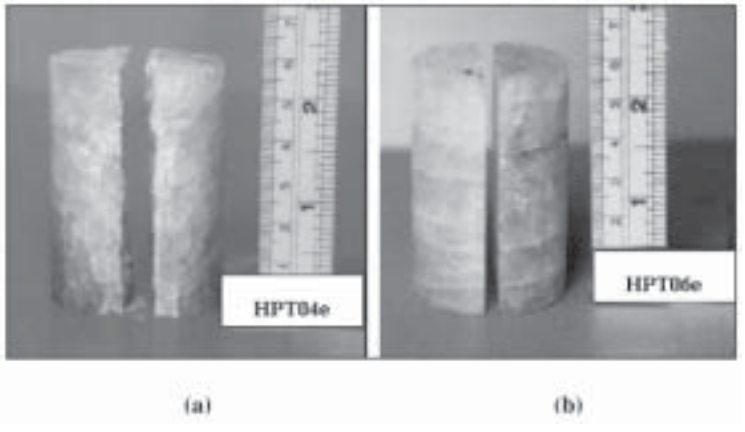

Figure 3. Specimens with tension-induced fracture (a) and with polished fracture (b)

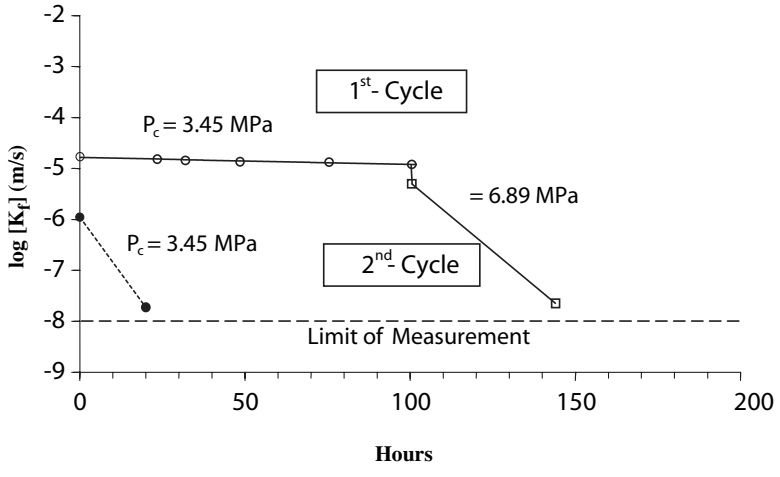

Figure 4. Hydraulic conductivity (K_f) of polished fracture under quasi-static loading. Two loading cycles are presented

shows the results of quasi-static loading test for some specimens.

For the static loading test, five specimens subjected to constant pressures of 0.69, 3.45, 6.98, 13.78 and 20.67 MPa. A power equation is used to fit the experimental results for each pressure level: $K_f = K_o (t)^{-b}$, where K_o represents the fracture permeability at time (t) equal to 1, and β is the time coefficient (Figure 6). The time coefficient β increases exponentially with the applied pressure (P_c): $\beta = 0.104 \cdot \exp(0.14\ P_c)$. This suggests that the reduction rate of fracture permeability is higher when the fracture is subjected to a greater pressure.

It was found that healing occurred for all tension-induced fractures after 120 h of loading (Figure 7). The Brazilian tensile strengths of each specimen measured before and after healing were compared to assess the healing effectiveness (H_e) of the fracture. Here H_e represents the percentage ratio of the fracture tensile strength (σ_H) to the intact tensile strength (σ_B) of the same salt specimen. The tensile failure occurred along the same plane that was induced before and after healing. Table 3 summarizes the results of the healing assessment test. The polished fractures could not be effectively healed even under the pressure of 6.89 MPa for 120 h. Healing was however found in all tension-induced fractures. Figure 8 shows the increase of H_e as the pressure (P_c) increases for the static loading test on tension-induced fractures.

Discussions and Conclusions

The assessment of fracture healing under radial loading has an advantage over that under normal (uniaxial) loading in terms of the maximum applied pressures. The applied axial load is limited by the compressive strength of the salt. The maximum axial stress used here was therefore limited to 7.8 MPa or about 30% of the strength. This is primarily to prevent the initiation of micro-cracks or fractures in the intact salt. For the radial loading test, the specimen can be subjected to a pressure as high as 20 MPa.

The occurrence of healing of salt fractures depends largely on the origin of the fractures. If a fracture is formed by separation or splitting of salt crystals, it can be easily healed even under

Table 3. Brazilian tension test results of dry salt specimens with tension-induced fractures and polished surfaces after healing under static and quasi-static loading

Specimen No.	Type of fracture	Radial pressure (MPa)	Test duration (h/step)	Brazilian tensile strength		Healing effectiveness
				Intact salt σ_B (MPa)	Salt with healed fracture, σ_H (MPa)	$H_e = (\sigma_H/\sigma_B) \times 100$ (%)
HPT01e	Tension	0.69	120	2.24	0.04	2
HPT02e	-	3.45	120	2.23	0.37	17
HPT03e	Induced	6.89	120	2.24	0.36	16
HPT04e	fracture	13.78	120	2.47	1.04	42
HPT05e		20.67	120	1.96	0.82	42
HPT06e	Polished	3.45	100	1.68	0.06	4
	surface	6.89				
HPT07e	Tension	3.45 →	96	1.30	1.24	94
HPT08e	-	6.89	24	2.50	1.97	79
HPT09e	induced	→ 10.34	24	2.23	1.17	53
	fracture	→ 13.78				

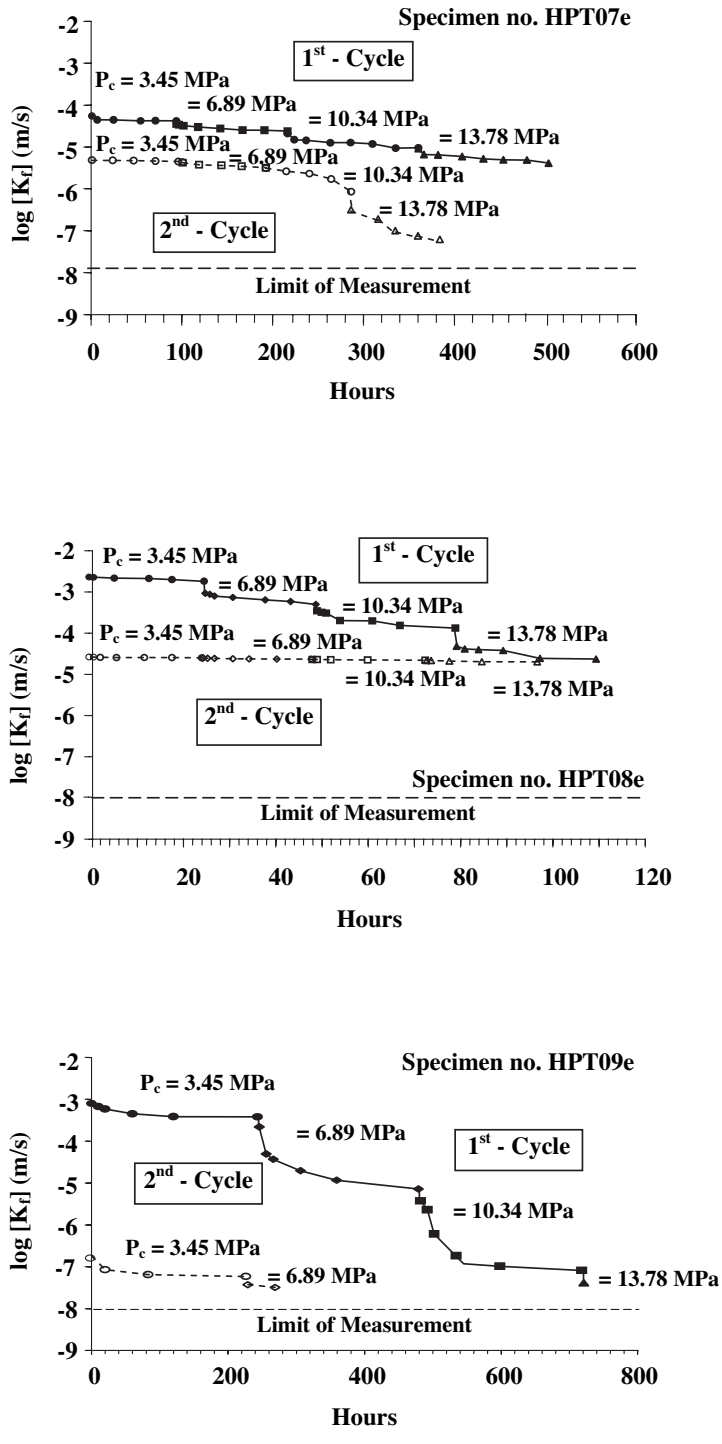

Figure 5. Hydraulic conductivity (K_f) of tension-induced fracture in three salt specimens as a function of time under quasi-static loading, for specimen * HPT07e (top), HPT08e (middle) and HPT09e (Bottom)**

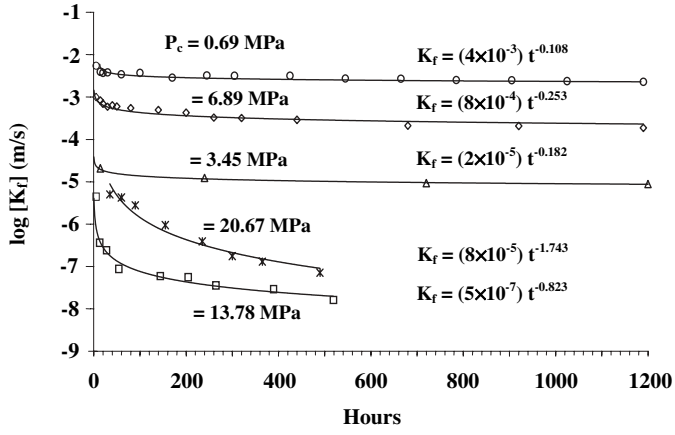

Figure 6. Hydraulic conductivity (K_f) of five tension-induced fractures as a function of time (t) under static loading

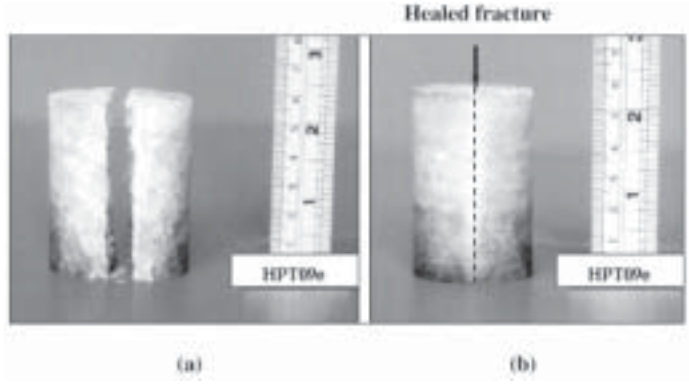

Figure 7. Tension-induced fracture in salt prepared by diameter loading, before healing (a) nad after healing (b)

relatively low stress for a short period. The splitting failure of salt crystals occurs by a separation of cleavage planes, which means that healing is likely to occur if the salt crystals on both sides of the cleavage plane return to their original position. For the fractures formed by separation of inter-crystalline boundaries, healing will not be easily achieved. In particular, if the fracture surface is coated with any inclusions, healing will not occur. This explains why the saw-cut fractures and polished fractures can not be effectively healed under the test conditions used here. It can be postulated here that healing of a fracture can be enhanced by the purity of the halite crystals on the opposite sides of the fracture. This is supported by the fact that the cleavage planes inside the salt crystal are purer than the inter-crystalline boundaries, and purer than the saw-cut and polished surfaces. These artificial surfaces could be contaminated during the preparation process. To heal a saw-cut or polished salt fracture, a much higher confinement and temperature than those used here may be required.

It is not clear from the experimental results that fractures under saturated brine can be healed more effectively than those under dry conditions. This is because the two test conditions are applied on the saw-cut fractures and with relatively low axial stresses. For the saturated

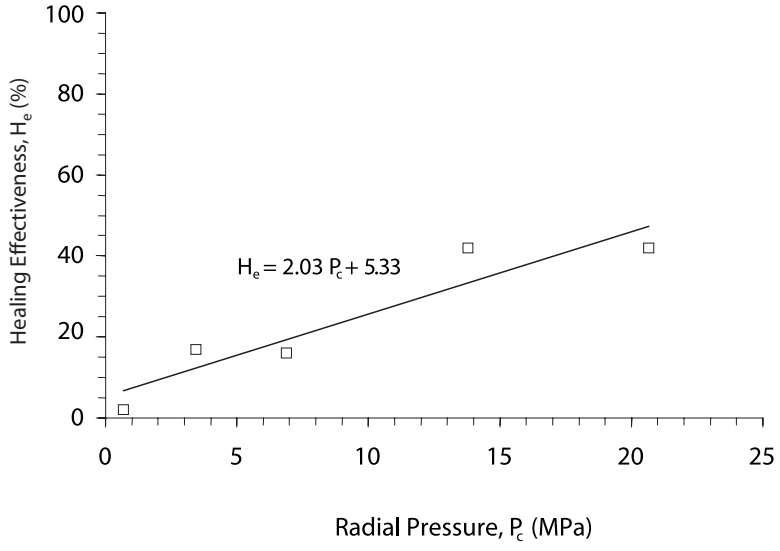

Figure 6. Healing effectiveness (H_e) as a function of radial pressure (P_c) for tension-induced fractures after healing for 120 h

testing, it was found that re-crystallization occurred in the fractures in the form of small salt crystals. Such a process however can not hold the fractures together. The specimens can be easily pulled apart by hands.

The results suggest that both pressure and time are important factors for the effectiveness of healing. The hydraulic conductivity for all salt fractures decreases with increasing applied pressure and time. This implies that fracture healing is accompanied by fracture closure. Both processes are time-dependent. The closure involves the visco-plastic deformation of the salt on both sides of the fracture. The healing involves a covalent bonding of the surfaces. It is permanent and remains even after the load has been removed. Owing to the surface smoothness, the polished fractures show a lower permeability than do the tension-induced fractures. This however does not necessarily mean that the polished fractures heal more effectively than do the tension-induced fractures. A reduction of fracture permeability does not necessarily mean that the healing has occurred. This is evidenced by the fact that even though the polished fracture has been compressed until its permeability becomes lower than 10^{-8} m/s, no healing has taken place in the fracture.

Since all fractures tested here are well mated, the impact of fracture roughness can not be truly assessed. More testing is needed to confirm any mathematical relationship between the healing effectiveness and the amount and type of inclusions. For the healing assessment method, a direct tension test could be used to minimize the impact of the stress gradient induced along the fracture plane. From the results obtained here, it can be postulated that under preferable conditions (stress state, time, temperature, purity, crystal orientation, etc.), a complete healing of salt fractures is possible.

Acknowledgment

This research is funded by Suranaree University of Technology. Permission to publish this paper is gratefully acknowledged.

References

Allemandou, X., and Dusseault, M.B. (1993). Healing processes and transient creep of salt rock. In: Geotechnical Engineering of Hard Soils-Soft Rocks. Balkema Publishers, Rotterdam, Netherlands, p. 1,581-1,590.

ASTM D2938-79. (1979). Standard Test Method for Unconfined Compressive Strength of Intact Rock Core Specimens. In: Annual Book of ASTM Standards. American Society for Testing and Materials, Philadelphia, 04.08.

ASTM D3967-81. (1981). Standard Test Method for Splitting Tensile Strength of Intact Rock Core Specimens. In: Annual Book of ASTM Standards. American Society for Testing and Materials, Philadelphia, 04.08.

ASTM D4543-85. (1985). Standard Practice for Preparing Rock Core Specimens and Determining Dimensional and Shape Tolerances. In: Annual Book of ASTM Standards. American Society for Testing and Materials, Philadelphia, 04.08.

ASTM D5731-95. (1995). Standard Test Method for Determination of The Point Load Strength Index of Rock. In: Annual Book of ASTM Standards. American Society for Testing and Materials, Philadelphia, 04.08.

Chan, K.S., Munson, D.E., Fossum, A.F., and Bodner, S.R. (1998). A constitutive model for representing coupled creep, fracture and healing in rock salt. Proceedings of the 4th Conference on the Mechanical Behavior of Salt; The Pennsylvania State University, June 17-18, 1996. Clausthal-Zellerfeld, Trans Tech Publications, Germany, p. 211-234.

Habib, P., and Berest, P. (1993). Rock mechanics for underground nuclear waste disposal in France. In: Comprehensive Rock Engineering. Hudson, J.A. (ed). Pergamon Press, Oxford, UK, (5):547-563.

Katz, D.L., and Lady, E.R. (1976). Compressed air storage for electric power generation. Dept. of Energy, Pacific Northwest, Richland, Washington.

Miao, S., Wang, M.L., and Schreyer, H.L. (1995). Constitutive models for healing of materials with application to compaction of crushed rock salt. J. of Engineering Mechanics. ASCE., 10(121):1,122-1,129.

Munson, D.E., Chan, K.S., and Fossum, A.F. (1999). Fracture and healing of rock salt related to salt caverns. SMRI Report, Spring Meeting, April 14-16, Las Vegas, Nevada. Solution Mining Research Institute, Encinitas, California.

Ouyang, S., and Daemen, J.J.K. (1989). Crushed salt consolidation. Technical Report NUREG/CR-5402, U.S. Nuclear Regulatory Commission, Washington, DC.

Renard, F. (1999). Pressure solution and crack healing and sealing. Institute of Geology and Department of Physics. Charles University, Prague; Summer school on: Geology related to nuclear waste disposal, July 5-11, Roztez, Czech Republic. University of Oslo, Norway.

Suwanich, P. (1986). Potash and rock salt in Thailand. Nonmetallic Minerals Bulletin No.2. Economic Geology Division, DMR, Bangkok, Thailand.

Warren, J. (1999). Evaporites: Their Evolution and Economics. Blackwell Science, Oxford, UK. 438 p.

Zeigler, T.W. (1976). Determination of rock mass permeability. Technical Report S-76-2, U.S. Army Engineer Waterways Experiment Station, Vicksburg, Mississippi.